Journal of Medicinal Chemistry

Article

pubs.acs.org/jmc

Binding Evaluation of Fragment-Based Scaffolds for Probing Allosteric Enzymes

Isabelle Krimm,*[,†] Jean-Marc Lancelin,[†] and Jean-Pierre Praly[‡]

[†]Institut des Sciences Analytiques, UMR CNRS 5280, Université de Lyon, Université Claude Bernard Lyon 1, Bât. CPE Lyon, Domaine scientifique de la Doua, F-69622 Villeurbanne, France

[‡]Equipe Chimie Organique 2-Glycochimie, Institut de Chimie et Biochimie Moléculaires et Supramoléculaires associé au CNRS, UMR 5246, Université de Lyon, Bâtiment Curien, 43 Boulevard du 11 Novembre 1918, F-69622 Villeurbanne, France

ABSTRACT: Fragment-based drug discovery has become a powerful method for the generation of drug leads against therapeutic targets. Beyond the identification of novel and effective starting points for drug design, fragments have emerged as reliable tools for assessing protein druggability and identifying protein hot spots. Here, we have examined fragments resulting from the deconstruction of known inhibitors from the glycogen phosphorylase enzyme, a therapeutic target against type 2 diabetes, with two motivations. First, we have analyzed the fragment binding to the multiple binding sites of the glycogen phosphorylase, and then we have investigated the use of fragments to study allosteric enzymes. The work we report illustrates the power of fragmentlike ligands not only for probing the various binding pockets of proteins, but also for uncovering cooperativity between these various binding sites.

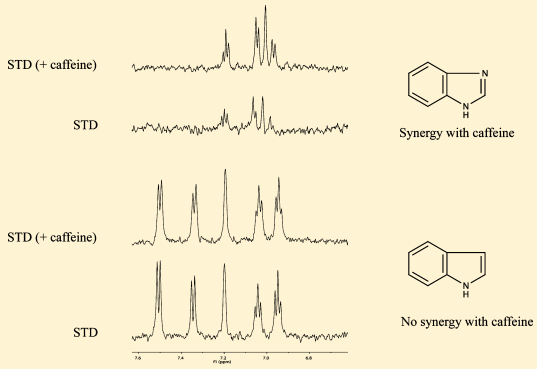

INTRODUCTION

The fragment-based approach constitutes a powerful method to design potent novel inhibitors against enzymes and protein−protein interactions.[1−4] Since its first application by Abbott in 1996,[5] this drug discovery process has successfully been used against some challenging targets,[6] and has gained a growing interest in both the pharmaceutical research and chemical biology fields.[7] In spite of their low complexity leading to weak affinity for their macromolecule target (K_D > 100 μM), fragments were shown to bind protein hot spots, focal points where binding energy is concentrated,[8] independent of their structure and affinity.[9,10] Interestingly, hit rates in fragment-based screening were reported to be correlated with the protein ability to bind druglike ligands with high affinity, which led to the proposal of fragment-based screening results as a tool to assess protein druggability.[9−13]

Fragments, as weak but efficient ligands,[14,15] constitute powerful tools to probe protein binding pockets. One of the methods published in the literature in the past five years consists of deconstructing known inhibitors into fragments.[16] Three studies have questioned the binding site evolution from a fragment to an inhibitor. In the group of Soichet, none of the fragments resulting from the deconstruction of a β-lactamase inhibitor were shown to recapitulate their position in the large inhibitor. The fragments were shown to explore new binding sites on the protein surface.[16] In another study, the dissection of the natural cyclopentapeptide argifin, a chinitase inhibitor, showed that the small molecules all retain a position similar to the one they had in the entire inhibitor.[17] Our group recently reported the deconstruction of Bcl-xL inhibitors, showing that the fragments have a preferred binding site (the protein hot spot). As a consequence, most of the fragments did not keep the binding site they occupy in the protein−inhibitor complex.[18] The question of the role of the ligand efficiency (the binding energy divided by the number of heavy atoms of a ligand, LE) was also addressed in different studies. In the group of Abell, the deconstruction method was used to probe hot spots at the NADPH-binding site of a dehydrogenase protein,[19] and to identify the parts of the cofactor contributing most to the binding energy. More recently, nicotinic acetylcholine receptor ligands were deconstructed, showing that ligand efficiencies of the fragments were correlated with their binding pocket; fragments binding hot spots had the highest LE.[20] The same group then studied protein−fragment interactions with fragments resulting from the deconstruction of three non-nucleoside inhibitors of HIV-1 reverse transcriptase.[21] Only the larger fragments were shown to bind to the protein. The LEs observed were significantly lower than the expected LEs, which could be compensated by taking into account the ligand-independent free energy (estimated to be 7 kcal·mol^{-1}).[21] For our part, we observed that fragments from Bcl-XL inhibitors did not systematically retain affinity for the protein.[18] This loss of affinity was poorly correlated with the fragment complexity or the predicted ligand efficiency of the fragment. By contrast, other fragments displayed affinities larger than expected, which illustrated that some parts of the ligands contribute more than

Received: October 25, 2011
Published: January 9, 2012

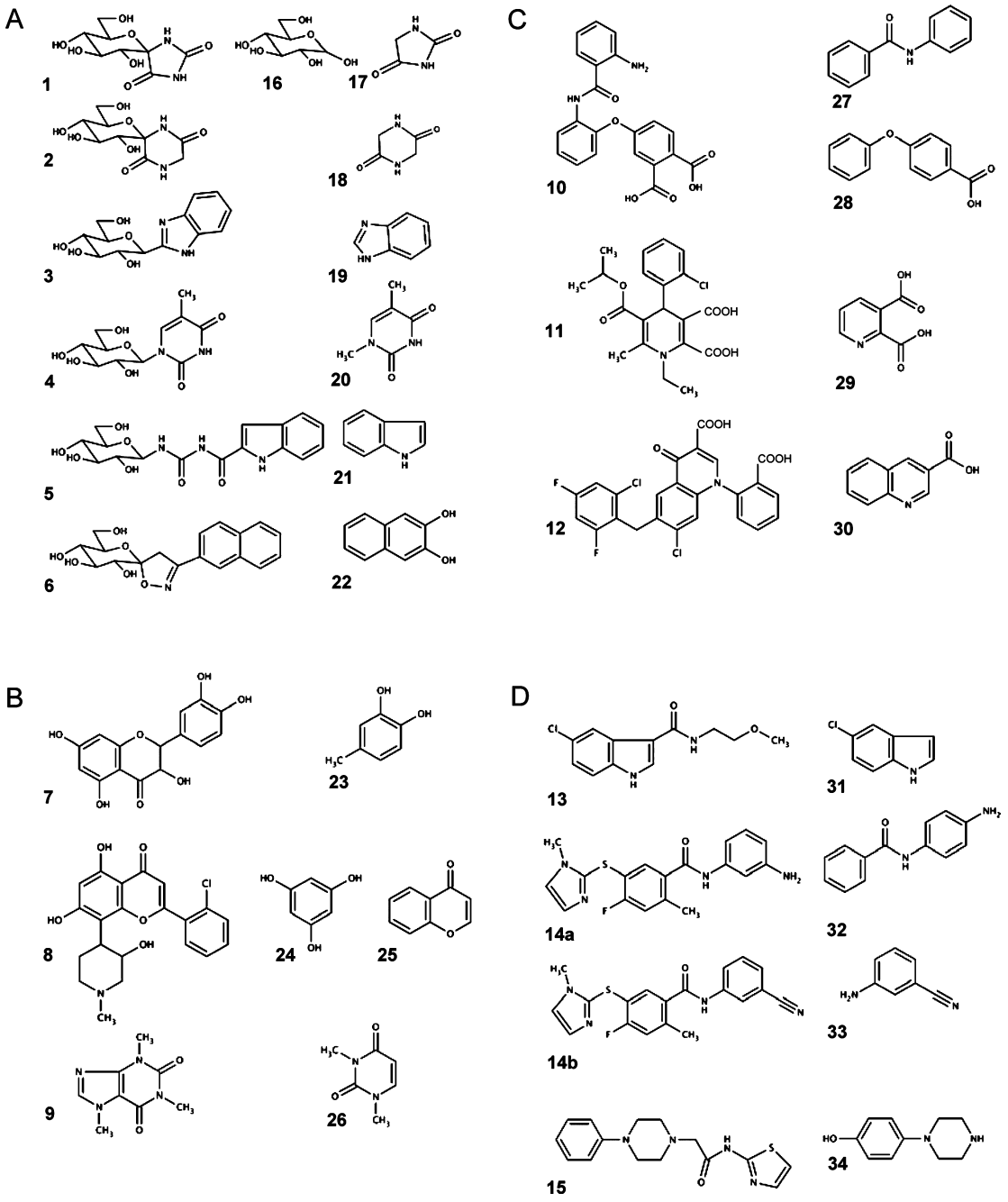

Figure 1. Fifteen GP inhibitors selected for deconstruction (**1**–**15**) and the corresponding 19 fragments selected for NMR analysis (**16**–**34**). (A) Inhibitors **1**–**6** target the active site. (B) Inhibitors **7**–**9** bind the inhibitor site. (C) Inhibitors **10**–**12** bind the allosteric site. (D) Inhibitors **13**–**15** bind the new allosteric site.

others to the overall affinity, as stated by the "group efficiency" concept.[22]

These reports demonstrate how fragment-based protein–ligand interactions help to better understand and anticipate the interactions between proteins and elaborated inhibitors. In the present work, we chose to investigate protein–fragment interactions with two major motivations. The first one was to examine the behavior of fragments when multiple binding pockets (and therefore multiple hot spots) can be targeted on the same protein. The second aim was to explore the use of fragmentlike molecules to study allosteric enzymes, where allosteric regulation is due to small-molecule binding. To address both questions, we studied fragment–protein interactions using the glycogen phosphorylase (GP) enzyme as a protein model.

The GP protein is the rate-limiting enzyme of glycogen degradation and as such has emerged as a potential therapeutic target for type 2 diabetes.[23,24] GP is an allosteric enzyme with six regulation sites, including a phosphorylation site where the inactive dephosphorylated form GPb is activated in the phosphorylated form GPa. The enzyme exists in two conformational states, the relaxed (R) state, which predominates in the GPa form, and the tensed (T) state; these states are intrinsically more active and less active, respectively.[23,25−28] A very large number of inhibitors/activators have been reported,[24−28] and positive homotropic as well as positive

dx.doi.org/10.1021/jm201439b | J. Med. Chem. 2012, 55, 1287−1295

Table 1. Expected LE and K_D of the 19 Fragments Resulting from the Deconstruction of 15 GP Inhibitors[a]

inhibitor	site[b]	IC_{50}[c]	HAC[d]	LE[e]	ref	fragment	HAC[d]	theoretical K_D[c]	binding[f]
1	A	3.1, RMGPb	17	0.44	25, 28	**16**	11	272	no
						17	7	5392	no
2	A	59.8, RMGPb	18	0.32	25	**18**	8	13263	no
3	A	8.6, RMGPb	20	0.34	25, 28	**19**	9	5254	yes
4	A	6.6, RMGPb	20	0.35	28	**20**	9	4664	no
5	A	4, RMGPb	26	0.28	28	**21**	9	13535	yes
6	A	0.63, RMGPb	25	0.34	25	**22**	12	1056	yes
7	B	4.8, RMGPa	22	0.33	28	**23, 24**	9	6670	yes
7	B	20.9, RMGPb	22	0.29	28	**23, 24**	9	12200	yes
8	B	1.2, RMGPb	28	0.29	28	**25**	11	4720	yes (GPa)
9	B	100, RMGPa.b	14	0.39	31	**26**	10	1390	no
10	C	1.3, HLGPa	31	0.26	32	**27**	15	1417	yes
						28	16	916	yes
10	C	0.9, RMGPb	31	0.27	32	**27**	15	1187	yes
						28	16	758	yes
11	C	0.0016, RMGPb	28	0.43	33	**29**	12	170	no
12	C	0.024, RMGPb	34	0.31	30	**30**	13	1220	yes
13	D	12.5, HLGPa	17	0.39	34	**21**	9	2536	yes
						31	10	1307	yes
14a	D	2.7, RMGPa	25	0.30	35	**27**	15	456	yes
						32	16	273	yes
14b	D	9.9, RMGPa	26	0.26	35	**33**	9	18523	yes
15	D	96.9, RMGPa	21	0.26	35	**34**	13	3276	yes (GPa)

[a]Binding of the fragments to the GP protein as observed by NMR is indicated. [b]Site A = active site, site B = inhibitor site, site C = allosteric site, and site D = new allosteric site. For inhibitors **14a**, **14b**, and **15**, the binding site has been proposed by docking and is not experimentally confirmed. [c]IC_{50} and K_D values are given in micromolar units. RMGPb = rabbit muscular GPb, and HLGPa = human liver GPa. [d]HAC = heavy atom count. [e]LE = ligand efficiency (kcal·atom^{-1}). [f]Binding observed by NMR experiments (this work).

and negative heterotropic effects have been observed between the various binding sites.[28−30,23,25,26] For the present study, we have analyzed fragment−GP interactions using 19 fragmentlike molecules resulting from the deconstruction of 15 distinct GP inhibitors.[24,27,29−36] Binding of these fragment-based scaffolds to the GP protein was evaluated using homonuclear 1D and 2D NMR experiments. In addition, eight fragment analogues were chosen to further characterize the fragment−GP interactions. Then, to examine fragment specificity and cooperativity effects, binding experiments were recorded in the presence of selected GP ligands.

This study, which investigates the behavior of fragments resulting from known inhibitors of a multiple-binding-site protein, illustrates the power of fragments to probe the binding pockets of proteins. In particular, our protein model demonstrates that simple fragmentlike ligands can be used to highlight synergy mechanisms observed in allosteric enzymes.

RESULTS

Deconstruction of Selected GP Inhibitors. A large number of inhibitors that target the GP protein in the micromolar to nanomolar range have been discovered for four binding pockets (the active site, the inhibitor site, the allosteric site, and the new allosteric site) out of the six sites of regulation of the enzyme.[23−34] Here, 15 GP inhibitors among the compounds exhibiting the highest ligand efficiencies have been selected (Figure 1). Inhibitors **1**−**6** bind the active site (named site A in Table 1), molecules **7**−**9** bind the inhibitor site (site B), compounds **10**−**12** bind the allosteric site (site C), and inhibitors **13**−**15** bind the so-called new allosteric site (site D) of the enzyme (Figure 1 and Table 1). A simple deconstruction approach was used to generate commercially available fragmentlike molecules. We did not use the prediction of the dissociation constant K_D as a criterion for the substructure selection since we and other groups observed that the ligand efficiency of fragments is not correctly predicted from the ligand efficiency of the large inhibitors.[18,20] Experimental solubility of the selected molecules was carefully checked by 1D NMR WaterLOGSY experiments at 500 μM to avoid false-positive results in the NMR binding experiments.[37] The 19 fragments (molecules **16**−**34**) resulting from the deconstruction of 15 GP inhibitors are displayed in Figure 1. The affinity, LE, and heavy atom count (HAC) of the inhibitors and the corresponding values calculated for the fragments are reported Table 1.

NMR Binding Experiments. Binding assays against both GPa and GPb proteins were achieved using NMR experiments. Fragments that retained affinity for the protein were identified using classical NMR 1D binding experiments (STD and WaterLOGSY),[36,37] in conditions similar to those of previous studies (Figure 2).[18] Fragments were considered as binders when both NMR experiments exhibited a binding signal. Binding of the molecules was also confirmed by 2D transferred NOESY experiments recorded in the presence of the protein (Figure 3).[39] Results for the binding evaluation of the fragments are reported in Table 1. Among the 19 fragments tested, 11 molecules were shown to bind both GPa and GPb proteins, whereas two molecules exhibited weak binding signals against GPa and no binding against GPb. STD factors f_{STD} were measured for all binders against both GPa and GPb (Table 2).[40] While the STD and WaterLOGSY factors are not a direct measurement of the ligand affinity, they represent very useful tools to rank the ligands.[18,40,41] Fragment **31** exhibits the largest f_{STD} with both GPa and GPb (Table 2), but the f_{STD}

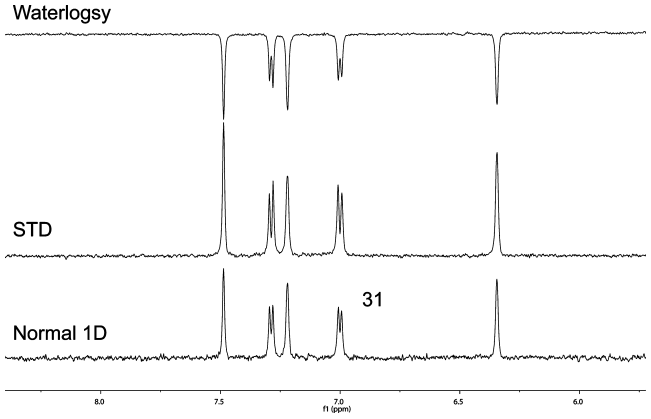

Figure 2. 1D ligand-observed NMR binding experiments. 1D spectrum, STD spectrum, and WaterLOGSY spectrum of 400 μM fragment **31** in the presence of 2 μM GPa.

value is significantly higher with GPa. Analysis of the ensemble of f_{STD} values shows binding differences for fragments **24**, **27**, and **32**, which preferentially bind GPa, whereas fragments **19** and **33** preferentially bind GPb. For the remaining fragments, no significant binding difference is observed between GPa and GPb.

Analogue Analysis. To analyze further the fragment−GP interactions, binding was characterized for eight additional fragmentlike molecules (molecules **35**−**42** in Figure 4). We compare analogues of fragments **17**, **21**, and **22**. Fragment **17** is a very small polar fragment that does not bind GP, while fragments **21** and **22** exhibit high f_{STD} values with both GPa and GPb (Table 2). Binding was analyzed by 1D STD and WaterLOGSY NMR experiments as well as 2D NOESY experiments.

Table 2. Ranking of the Fragments Based on 1D NMR Binding Experiments[a]

fragment	f_{STD}(GPa)	ranking for GPa	f_{STD}(GPb)	ranking for GPb
31	36.3−45	1	11.7−15.8	1
32	17.8−29.5	2	2.1−2.8	13
22	22.7−23.3	3	13.2−14.3	2
21	17−22.7	4	12.6−13.4	3
24	22	5	4.7	9
27	15−21.4	6	1.5−3.6	12
28	10.5−17.5	7	2.2−4.9	8
23	11.8−16	8	6.3−7.6	5
30	9.2−15.6	9	1.7−4.7	10
35	10−13.3	10	3.2−4	11
42	10−12.8	11	3.3−7	7
19	2.7−9.2	12	2.9−8.9	4
25	4.5−7.1	13	0	
33	6.1−6.7	14	6−6.7	6
34	3.9	15	0	

[a]STD factors f_{STD} are measured for each of the aromatic resonances of the molecules. The minimal and maximal values are reported for each fragment.

All compounds **35**−**42** bind both GPa and GPb. The f_{STD} values of **19**, **35**, **36**, and **37** (analogues of **21**) indicate that the number and the position of nitrogen atoms have a significant effect on binding (Figure 4). By contrast, analysis of **38**, **39**, and **40** (analogues of **22**) shows that the position of the hydroxyl functions has no impact on the interaction. Finally, fragments

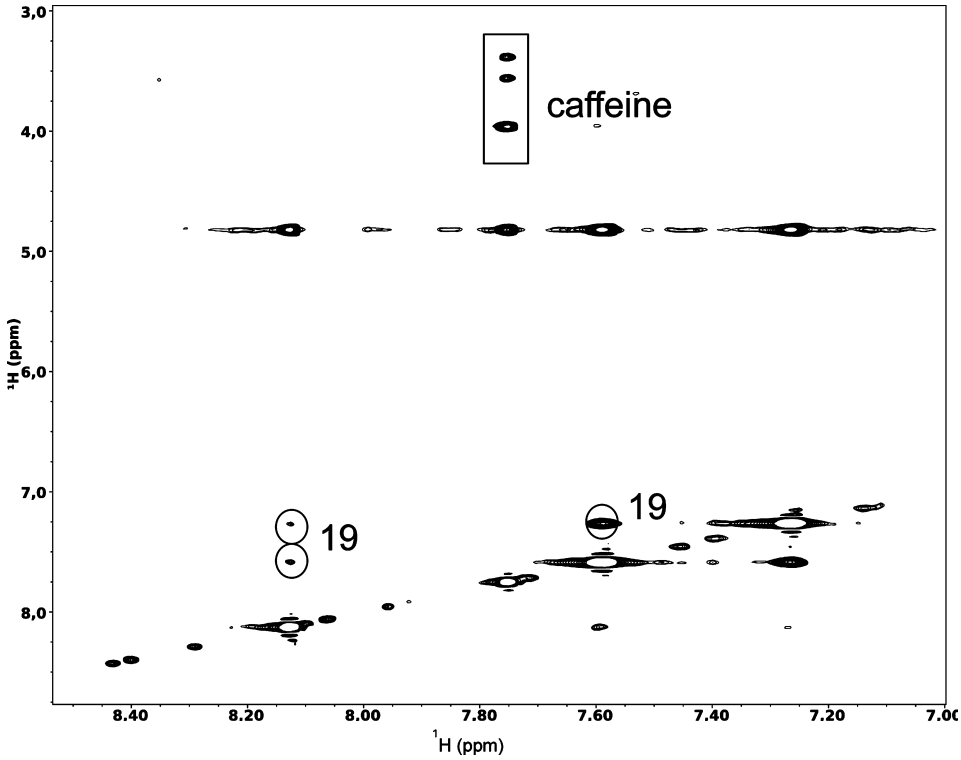

Figure 3. 2D ligand-observed NMR binding experiments. Portion of the ^{1}H,^{1}H NOESY spectrum of **19** (1 mM) and caffeine **9** (1 mM) in the presence of GPb (50 μM). Transferred NOE peaks due to binding to the protein are displayed with circles for **19** and with a rectangular frame for caffeine.

dx.doi.org/10.1021/jm201439b | J. Med. Chem. 2012, 55, 1287−1295

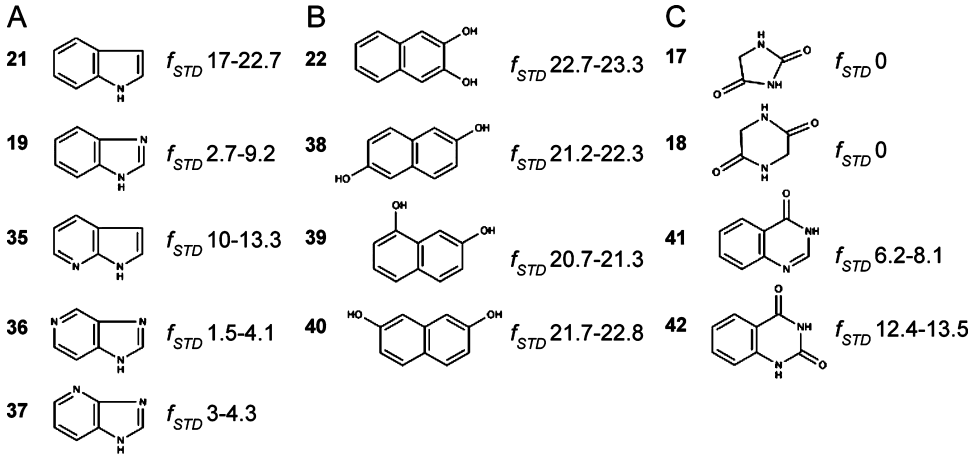

Figure 4. Binding analysis of fragments and analogues: (A) analogues of fragment **21**, (B) analogues of fragment **22**, (C) analogues of fragments **17** and **18**. The f_{STD} values are indicated for each fragment.

Table 3. Perturbations (%) of the STD Factor Values f_{STD} of the Fragments upon Addition of Inhibitor 6, Caffeine 9, AMP, and Fragment 31[a]

	inhibitor **6**		caffeine		AMP		fragment **31**	
fragment	GPa	GPb	GPa	GPb	GPa	GPb	GPa	GPb
19	+50	−25	+65		−60	−30	−45	−90
21		−30					−80	−85
22		−25						
24	−75	−65	−40	−50				−35
28	+35	−30	+30	−30			+50	
30			−40	−90	−40	−40	−40	−60
31								
32	−50		−30	−35	−30		−40	
33	+100		+100		−45	−45	−90	−85
35					−30	+30	−30	
42	+30		−45	−60	−45	−40	+30	

[a]Effects observed with GPa and GPb are indicated. Inhibitor **6**, caffeine, AMP, and fragment **31** bind respectively the active site, the inhibitor site, the allosteric site, and the new allosteric site. Positive numbers indicate that the fragment f_{STD} increases in the presence of the ligand; negative numbers indicate that the fragment f_{STD} decreases in the presence of the ligand. Values correspond to the average modification observed for the aromatic resonances of the fragments. Only perturbations >25% are reported. The fragment concentration is 400 μM, the ligand concentration is 1−2 mM, and the protein concentration is 2 μM.

41 and **42** similar to fragments **17** and **18** were tested. Clearly, the addition of an aromatic moiety enhances the affinity for the enzyme.

Binding Experiments in the Presence of GP Ligands. 1D NMR binding experiments of ten fragments selected for their high f_{STD} factors were compared in the absence and the presence of three known GP ligands and fragment **31**. The three GP ligands are the active site inhibitor **6**, caffeine **9**, which binds GP at the inhibitor site, and adenosine monophosphate AMP, which binds the allosteric site. Fragment **31**, resulting from inhibitor **13**, exhibits the highest f_{STD} value among the fragments analyzed. According to competition experiments, **31** binds the new allosteric site, as expected from the original inhibitor (Table 3). The motivations for these experiments were to study the fragment specificity, identify the binding site(s) of the fragments, and observe cooperativity effects between the ligands.

Glucose was previously shown to bind GP in synergy with caffeine,[42] due to the ability of both molecules to stabilize the protein T state. To validate the use of f_{STD} values as an indicator of synergy effects, we measured the f_{STD} factors of caffeine in the presence and the absence of glucose against both GPa and GPb. The f_{STD} value of caffeine in the presence of 50 mM glucose strongly increases (+140%) with GPa (glucose promotes the T state), whereas no change is observed with GPb (the T state is predominant) (Figure 5A).

In the experimental conditions, competition and/or a negative heterotropic effect are indicated by a decrease of the fragment STD signal in the presence of the second ligand, whereas synergy is indicated by an increase of the fragment STD signal in the same conditions. As reported in Table 3, very different results are obtained for the 10 fragments. Moreover, effects detected can be different for GPa or GPb (Table 3 and Figure 5). As an example, while synergy is observed for fragments **19** and **33** with both inhibitor **6** and caffeine in the presence of GPa but not GPb (Figure 5B,C), f_{STD} values of **19** and **33** decrease with **31** in the presence of both GPa and GPb. By contrast, no significant effects are noticed for **22**, **28**, and **35**, whereas fragments **24** and **32** are mostly perturbed by the presence of inhibitor **6** and caffeine (see Figure 5D). Regarding the indole **21**, the fragment binding strongly decreases with the addition of the chloroindole **31**, indicating that **21** binds the new allosteric site, as expected from the original inhibitors such as **13**.

dx.doi.org/10.1021/jm201439b | J. Med. Chem. 2012, 55, 1287−1295

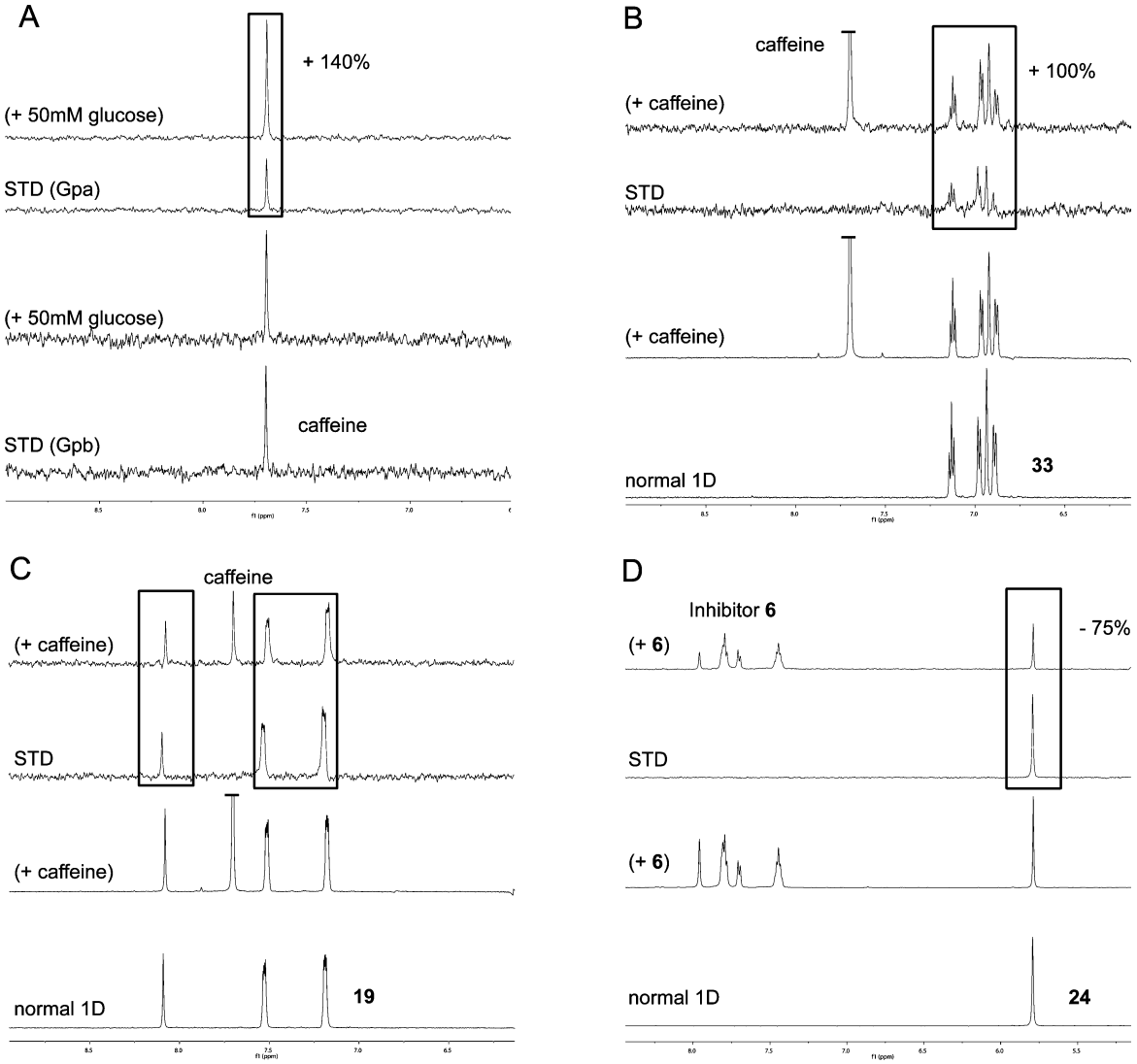

Figure 5. Allosteric interactions between molecules. (A) Synergy is observed between caffeine **9** (400 μM) and glucose **16** (50 mM) with GPa (2 μM) but not GPb (2 μM). (B) Synergy is observed between fragment **33** (400 μM) and caffeine **9** (2 mM) with GPa (2 μM). (C) No synergy is observed between fragment **19** (400 μM) and caffeine **9** (2 mM) with GPb (2 μM). (D) Addition of inhibitor **6** (1 mM) induces a drop in intensity in the STD spectrum of fragment **24** (400 μM) with GPa (2 μM).

DISCUSSION

In the present work, we have analyzed the binding properties of fragmentlike molecules resulting from the deconstruction of inhibitors targeting four binding sites of the GP protein, an enzyme with multiple sites of regulation.[23−28] The aim of the study was to investigate two main issues: the behavior of fragments in a protein with multiple binding pockets and the use of fragments to study allosteric enzymes.

Nineteen fragments resulting from the deconstruction of 15 inhibitors were tested against GP. Only 11 of the fragments retained affinity for the protein (Tables 1 and 2). Considering that the LE is conserved from the fragment to the inhibitor, the expected fragment K_D was calculated to vary from 170 μM to 18.5 mM (Table 1). Clearly, a poor correlation is observed between the expected binding and the binding measured by NMR (see Table 1 and f_{STD} values reported in Table 2). As an example, fragments **23**, **24**, and **33**, which were not predicted to bind (K_D = 6.6 and 18.5 mM, respectively), are observed as binders, whereas fragments **16** and **29** (predicted K_D = 0.27 and 0.17 mM) do not bind the protein. While fragments to be followed-up are not necessarily the fragments with the higher LE,[43] one of the objectives in the fragment-based drug discovery (FBDD) process is to keep the LE constant while the fragment is processed to the inhibitor.[44] However, as confirmed here, deconstruction studies show that the LE is not equally spread in the inhibitors, and fragments with LE higher than expected are likely to bind a hot spot of the protein pocket.[18−20,22]

Recently, the size of the fragments was reported to be a critical parameter for binding.[21] In our study, binders (average HAC = 12.8) are larger than nonbinders (average HAC = 9.5), but very small fragments containing an aromatic moiety (HAC $\leq$ 9) are capable of binding the GP protein (see fragments **23**, **24**, and **33**). By contrast, very small polar fragments (**17**, **18**, and **20**) do not bind GP, unless an aromatic moiety is added (see fragments **41** and **42** derived from **17** in Figure 4). As recently reviewed, polar interactions are directional but do not always add much to the binding energy unless the interactions are well optimized.[45] For such polar groups, the cost of

dx.doi.org/10.1021/jm201439b | J. Med. Chem. 2012, 55, 1287−1295

desolvating is high and binding is observed only if a good match exits between the fragment and the protein binding pocket.

Another point highlighted by the analysis of fragment analogues concerns the structure−activity relationship (SAR) effects. As illustrated in Figure 4, a small modification of fragment **21** induces significant binding modification (see fragments **19**, **35**, **36**, and **37**). This SAR effect is not observed when **22** is compared to fragments **38**, **39**, and **40**. These observations concur with the competition experiments reported in Table 3. For fragment **22**, no specific binding site was observed. Fragment **22** binds through nondirectional hydrophobic interactions and can accommodate a variety of binding sites, which supports the absence of an SAR effect. The binding of **21** is more specific (new allosteric site D), and addition of nitrogen atoms modifies the interaction with GP (Figure 4).

What do the fragments reveal about the GP binding pockets? According to the competition experiments, only fragments **24** and **32** bind to the active site (Table 3). In addition, the rankings against GPa and GPb indicate that both fragments preferentially bind GPa over GPb. These results suggest that **24** and **32** bind to the relaxed form R of the enzyme, where the active site is accessible, and not to the tensed form T, where the active site is obstructed (see Table 2).[23−28] By analogy with glucopyranosyl inhibitors,[24,25,27] **24** is likely to bind GP via its hydroxyl functions, supporting the presence of a hot spot involving polar interactions in the GP active site (Figure 6A).

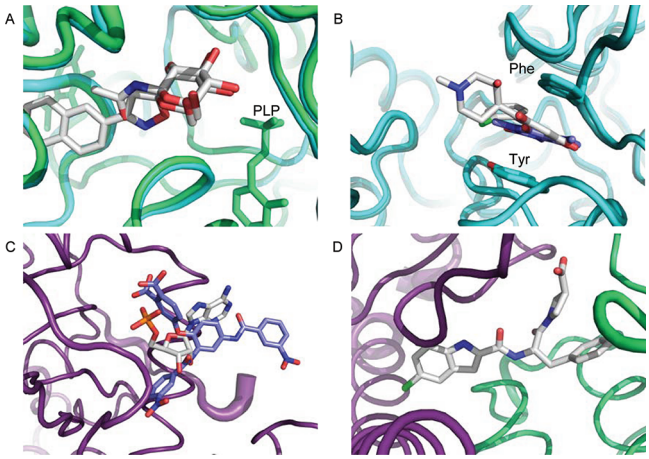

Figure 6. Binding modes of GP inhibitors in the (A) active site, (B) inhibitor site, (C) allosteric site, and (D) new allosteric site. (A) Structures of GBb in complex with inhibitor **6** (PDB code 2QRP) and GPa in complex with *N*-acetyl-*β*-D-glucopyranosylamine (PDB code 1L5Q). The cofactor pyridoxal phosphate PLP present in the GPa structure is displayed. (B) Structures of GPa in complex with flavopiridol **8** (PDB code 1C8K) and caffeine **9** (PDB code 1C8L). The GP aromatic residues involved in the compound binding are displayed. (C) Structures of GPa in complex with AMP (PDB code 1FA9) and an inhibitor analogous to **10** (PDB code 1Z6Q). (D) Structure of GPa complexed with a chloroindole-containing inhibitor, CP-403700, analogous to **13** (PDB code 1L5Q). One monomer is colored purple, and the second monomer is colored green.

Regarding the inhibitor site B, flavopiridol **8** and caffeine **9** both bind this hydrophobic binding pocket through stacking interactions with GP aromatic residues (Figure 6B).[46] A poor selectivity was observed with elaborated ligands,[46] and a similar observation was obtained here with the fragment molecules. As illustrated in Figure 6C, structural studies show that the AMP site inhibitors exhibit various binding modes. The allosteric site C is highly flexible,[32,26] which may partly rationalize the fact that site C is not recognized as a hot spot by the fragments used here. Finally, the new allosteric site D binds fragment **31** with high specificity. Site D contains a hydrophobic pocket that houses the chloroindole moiety **31** of inhibitor **13** and analogues (Figure 6D).[33,47] The indole ring is involved in hydrogen bonding and electrostatic interaction with the GP protein, which corroborates the observation that the nitrogen atom position affects the protein−ligand interactions (Figure 4 and Table 3). To summarize, these results show that fragments are capable of hitting particular hot spots in a protein with multiple binding pockets, highlighting the nature of the contacts involved in the protein−inhibitor complexes.

Another issue we address here is the use of fragments as probes to analyze allosteric sites in proteins. Allosteric sites are fundamental for protein functions, as they can control (inhibit or activate) the protein activity. The identification of allosteric sites[48] has an important impact in the context of drug design; allosteric sites may present advantages for druglike molecule binding over active sites. Moreover, knowledge of allosteric interactions is required to measure K_I with biological significance. The use of fragment-based screening to design novel molecules targeting allosteric sites has been recently reported.[7] We hereby report results proving that fragments are powerful tools to study the mechanism involved in the allosteric regulation, using the GP protein as a model.

The GP protein contains six potential regulatory sites sparsely located on the protein 3D structure: the catalytic site that binds the substrate glycogen and inhibitors based on glucose structure, the inhibitor site where caffeine binds, the Ser14 phosphorylation site, the allosteric site where AMP binds, the glycogen site, and the new allosteric site located at the dimer interface.[23,25−27] Phosphorylation of Ser14 and allosteric ligands such as AMP promotes the R state, whereas other ligands such as glucose and caffeine stabilize the less active T state.[23]

As reported in Table 3, synergy is observed between inhibitor **6** and both fragments **19** and **33** with GPa but not with GPb. Similarly, synergy is observed between caffeine **9** and both fragments **19** and **33** with GPa but not GPb (Figure 5B,C). This indicates that fragments **19** and **33** preferentially bind the protein T state stabilized by inhibitor **6** and caffeine. Fragments **19** and **33** also display a significant STD drop in the presence of **31**, showing that the binding site of the fragments is located in the new allosteric site where the chloroindole **31** binds. These observations match the synergy reported between chloroindole-containing inhibitors and both glucose and caffeine.[33,47] By contrast, **21** (indole) and **31** (chloroindole), which both bind the new allosteric site, do not bind synergistically with caffeine or inhibitor **6** (Table 3). This suggests that both fragments preferentially bind the R state. In agreement, **31** was shown to bind GPa tighter than GPb. According to the structural studies, the synergy observed between the elaborated inhibitors and glucose/caffeine is due to structural changes induced upon inhibitor binding at the dimer interface that stabilize the T state.[33,47] In the crystal structures, the chloroindole moiety is shown to interact only with one GP monomer (see Figure 6D). As a consequence, **31** binding should not modify the protein quaternary structure nor induce allosteric effects, as observed by NMR. This implies that the synergy effects observed with chloroindole-containing inhibitors are not due to the chloroindole moiety but to the additional moiety. Morover, **19** has a binding mode differing

dx.doi.org/10.1021/jm201439b | J. Med. Chem. 2012, 55, 1287−1295

from those of **21** and **31**, leading to different allosteric effects. Such opposite allosteric effects have been reported for ligands binding at the allosteric site C of the GP protein: inhibitors such as **10**−**12** synergistically bind with caffeine due to the stabilization of the protein T state,[49] while AMP binds at the same site and stabilizes the R state (Figure 6C)

CONCLUSION

We have investigated the binding of fragments resulting from previously developed glycogen phosphorylase inhibitors using NMR. This work illustrates that (1) SAR effects observed for a fragment are a good indicator that the fragment recognizes a protein hot spot, (2) fragments appear as valuable tools to probe the multiple binding pockets of proteins and highlight the nature of the contacts involved in the protein−ligand complexes, and (3) fragments can be used to analyze the synergy between ligands of various binding sites. One may anticipate that defragmentation of allosteric inhibitors will provide both conserved and nonconserved interactions between ligands, so that fragment-based studies of allosteric processes will help interpret the key interactions involved in allosteric regulation.

EXPERIMENTAL SECTION

Organic Fragments and Protein Samples. The fragments were obtained from Sigma-Aldrich or Acros and used without further purification. Aqueous solubility was checked for the compounds by recording the ^{1}H 1D NMR spectrum and WaterLOGSY spectrum at 500 μM.[37] Molecules for which autoassociation was observed from the WaterLOGSY signals were rejected. The selected compounds were stocked in 110 mM DMSO-d_6 solutions and conserved at −20 °C. Glycogen phosphorylases a and b were directly purchased from Sigma (CAS 9032-10-4 and 9012-69-5). The soluble protein concentration upon ligand addition was checked by recording the ^{1}H 1D NMR spectrum of 2 μM protein in the absence and the presence of 400 μM fragment, in 25 mM phosphate buffer, pH 7.0, using the integration of the protein NMR signals at 0.6 ppm. In addition, we checked that the binding of inhibitor **8** (flavopiridol) was not modified upon 400 μM fragment addition, using STD[38] and WaterLOGSY[37] experiments.

1D Ligand-Observed NMR Experiments. All spectra were acquired at 20 °C with a Varian Inova 600 MHz NMR spectrometer, equipped with a standard 5 mm triple-resonance inverse probe with a z-axis field gradient, actively shielded, and with an autosampler robot. The NMR tubes were prepared with 2 μM protein and 400 μM fragments in 25 mM phosphate buffer, pH 7.0. Control 1D normal and WaterLOGSY ^{1}H spectra preceded all experiments to assess the purity and stability of the fragments. 1D STD[38] and WaterLOGSY[37] experiments were run using parameters similar to those previously described.[19] The number of scans was set to 32, 800, and 128 for normal 1D, STD, and WaterLOGSY experiments. All NMR spectra were processed with the Varian VnmrJ software.

STD Factor Measurement. For quantitative analyses of STD spectra, the STD amplification factors f_{STD} were derived from the equation

$$f_{STD} = \frac{I_{STD}[L]_{tot}}{I_0[P]_{tot}}$$

where I_{STD} and I_0 are peak integrals in the STD and 1D experiments, respectively, and $[L]_{tot}$ and $[P]_{tot}$ are the total concentrations of the ligand and protein, respectively. $[L]_{tot}$ was 400 μM, and $[P]_{tot}$ was 2 μM. For the experiments in the presence of an additional ligand, the concentration was set to 2 mM for caffeine **9**, AMP, and fragment **31** and 1 mM for inhibitor **6**. 1D and STD experiments were performed in the same experimental conditions (spin lock, interscan delays), and parameters for the STD experiments (saturation frequency, saturation time) were identical for all samples. The number of scans was set to 800 and 1600 for the 1D and STD experiments, respectively. STD signals were measured for all protons in the aromatic region. The minimal and maximal values are reported in Table 2 and Figure 4. All experiments were repeated twice (with two different samples). Error in the STD amplification factors f_{STD} was estimated to be 20%. As a consequence, only perturbations larger than 25% are reported. Moreover, to avoid overinterpretation of the data, only effects larger than 50% are discussed.

2D Ligand-Observed NMR Experiments. NOESY experiments were recorded with a sample containing the GPa or GPb protein (50 μM) and the fragments (1000 μM) in 25 mM phosphate buffer. The mixing time was set to 600 ms.[39] In addition, experiments were recorded in the absence of the protein to avoid artifacts due to molecule aggregation.

AUTHOR INFORMATION

Corresponding Author

*Fax: +33-472431395. E-mail: isabelle.krimm@univ-lyon1.fr.

ACKNOWLEDGMENTS

We thank David Goyard at the University of Lyon (Equipe Chimie Organique 2-Glycochimie, Institut de Chimie et Biochimie Moléculaires et Supramoléculaires, UMR CNRS 5246) for providing compound **6** and Evangelia D. Chrysina for helpful discussion. We thank the Agence Nationale de la Recherche (funding of Project ANR-08-BLAN-0305, GPdia) for support of this work.

ABBREVIATIONS USED

AMP, adenosine monophosphate; GP, glycogen phosphorylase; HAC, heavy atom count; NMR, nuclear magnetic resonance; PDB, Protein Data Bank; STD, saturation transfer difference; WaterLOGSY, water ligand observed via gradient spectroscopy

REFERENCES

(1) Hajduk, P. J.; Greer, J. A decade of fragment-based drug design: strategic advances and lessons learned. *Nat. Rev. Drug Discovery* **2007**, *6*, 211−219.

(2) Congreve, M.; Chessari, G.; Tisi, D.; Woodhead, A. J. Recent developments in fragment-based drug discovery. *J. Med. Chem.* **2008**, *51*, 3661−3680.

(3) Zartler, E. D.; Shapiro, M. J. *Fragment-Based Drug Discovery: A Pratical Approach*; John Wiley & Sons, Ltd.: New York, 2008; p 296.

(4) Erlanson, D. A. Introduction to fragment-based drug discovery. *Top. Curr. Chem.* **2011**, 1−32.

(5) Shuker, S. B.; Hajduk, P. J.; Meadows, R. P.; Fesik, S. W. Discovering high-affinity ligands for proteins: SAR by NMR. *Science* **1996**, *274*, 1531−1534.

(6) Coyne, A. G.; Scott, D. E.; Abell, C. Drugging challenging targets using fragment-based approaches. *Curr. Opin. Chem. Biol.* **2010**, *14*, 299−307.

(7) Jahnke, W.; Rondeau, J. M.; Cotesta, S.; Marzinzik, A.; Pellé, X.; Geiser, M.; Strauss, A.; Gotte, M.; Bitsch, F.; Hemmig, R.; et al. Allosteric nonbisphosphonate FPPS inhibitors identified by fragment-based discovery. *Nat. Chem. Biol.* **2010**, *6*, 660−666.

(8) DeLano, W. L. Unraveling hot spots in binding interfaces: progress and challenges. *Curr. Opin. Struct. Biol.* **2002**, *12*, 14−20.

(9) Hajduk, P. J.; Huth, J. R.; Tse, C. Predicting protein druggability. *Drug. Discovery Today* **2005**, *10*, 1675−1682.

(10) Hajduk, P. J.; Huth, J. R.; Fesik, S. W. Druggability indices for protein targets derived from NMR-based screening data. *J. Med. Chem.* **2005**, *48*, 2518−2525.

(11) Keller, T. H.; Pichota, A.; Yin, Z. A practical view of 'druggability'. *Curr. Opin. Chem. Biol.* **2006**, *10*, 357−361.

(12) Huang, N.; Jacobson, M. P. Binding-site assessment by virtual fragment screening. *PLoS ONE* **2010**, 5:e10109.

(13) Barelier, S.; Krimm, I. Ligand specificity, privileged substructures and protein druggability from fragment-based screening. *Curr. Opin. Chem. Biol.* **2011**, *15*, 469−474.
(14) Kuntz, I. D.; Chen, K.; Sharp, K. A.; Kollman, P. A. The maximal affinity of ligands. *Proc. Natl. Acad. Sci U.S.A.* **1999**, *96*, 9997−10002.
(15) Bembenek, S. D.; Tounge, B. A.; Reynolds, C. H. Ligand efficiency and fragment-based drug discovery. *Drug Discovery Today* **2009**, *14*, 278−283.
(16) Babaoglu, K.; Shoichet, B. K. Deconstructing fragment-based inhibitor discovery. *Nat. Chem. Biol.* **2006**, *2*, 720−723.
(17) Andersen, O. A.; Nathubhai, A.; Dixon, M. J.; Eggleston, I. M.; van Aalten, D. M. Structure-based dissection of the natural product cyclopentapeptide chitinase inhibitor argifin. *Chem. Biol.* **2008**, *15*, 295−301.
(18) Barelier, S.; Pons, J.; Marcillat, O.; Lancelin, J. M.; Krimm, I. Fragment-based deconstruction of Bcl-xL inhibitors. *J. Med. Chem.* **2010**, *53*, 2577−2588.
(19) Ciulli, A.; Williams, G.; Smith, A. G.; Blundell, T. L.; Abell, C. Probing hot spots at protein-ligand binding sites: a fragment-based approach using biophysical methods. *J. Med. Chem.* **2006**, *49*, 4992−5000.
(20) de Kloe, G. E.; Retra, K.; Geitmann, M.; Källblad, P.; Nahar, T.; van Elk, R.; Smit, A. B.; van Muijlwijk-Koezen, J. E.; Leurs, R.; Irth, H.; Danielson, U. H.; de Esch, I. J. Surface plasmon resonance biosensor based fragment screening using acetylcholine binding protein identifies ligand efficiency hot spots (LE hot spots) by deconstruction of nicotinic acetylcholine receptor α7 ligands. *J. Med. Chem.* **2010**, *53*, 7192−7201.
(21) Brandt, P.; Geitmann, M.; Danielson, U. H. Deconstruction of non-nucleoside reverse transcriptase inhibitors of human immunodeficiency virus type 1 for exploration of the optimization landscape of fragments. *J. Med. Chem.* **2011**, *54*, 709−718.
(22) Verdonk, M. L.; Rees, D. C. Group efficiency: a guideline for hits-to-leads chemistry. *ChemMedChem* **2008**, *3*, 1179−1180.
(23) Agius, L. Physiological control of liver glycogen metabolism: lessons from novel glycogen phosphorylase inhibitors. *Mini-Rev. Med. Chem.* **2010**, *10*, 1175−1187.
(24) Praly, J. P.; Vidal, S. Inhibition of glycogen phosphorylase in the context of type 2 diabetes, with focus on recent inhibitors bound at the active site. *Mini-Rev. Med. Chem.* **2010**, *10*, 1102−1126.
(25) Chrysina, E. D. The prototype of glycogen phosphorylase. *Mini-Rev. Med. Chem.* **2010**, *10*, 1093−1101.
(26) Loughlin, W. A. Recent advances in the allosteric inhibition of glycogen phosphorylase. *Mini-Rev. Med. Chem.* **2010**, *10*, 1139−1155.
(27) Oikonomakos, N. G.; Somsák, L. Advances in glycogen phosphorylase inhibitor design. *Curr. Opin. Invest. Drugs* **2008**, *9*, 379−395.
(28) Johnson, L. N. Glycogen phosphorylase: control by phosphorylation and allosteric effectors. *FASEB J.* **1992**, *6*, 2274−2282.
(29) Anderka, O.; Loenze, P.; Klabunde, T.; Dreyer, M. K.; Defossa, E.; Wendt, K. U.; Schmoll, D. Thermodynamic characterization of allosteric glycogen phosphorylase inhibitors. *Biochemistry* **2008**, *47*, 4683−4691.
(30) Sprang, S.; Fletterick, R.; Stern, M.; Yang, D.; Madsen, N.; Sturtevant, J. Analysis of an allosteric binding site: the nucleoside inhibitor site of phosphorylase alpha. *Biochemistry* **1982**, *21*, 2036−2048.
(31) Kristiansen, M.; Andersen, B.; Iversen, L. F.; Westergaard, N. Identification, synthesis, and characterization of new glycogen phosphorylase inhibitors binding to the allosteric AMP site. *J. Med. Chem.* **2004**, *47*, 3537−3545.
(32) Zographos, S. E.; Oikonomakos, N. G.; Tsitsanou, K. E.; Leonidas, D. D.; Chrysina, E. D.; Skamnaki, V. T.; Bischoff, H.; Goldmann, S.; Watson, K. A.; Johnson, L. N. The structure of glycogen phosphorylase b with an alkyldihydropyridine-dicarboxylic acid compound, a novel and potent inhibitor. *Structure* **1997**, *5*, 1413−1425.
(33) Rath, V. L.; Ammirati, M.; Danley, D. E.; Ekstrom, J. L.; Gibbs, E. M.; Hynes, T. R.; Mathiowetz, A. M.; McPherson, R. K.; Olson, T. V.; Treadway, J. L.; Hoover, D. J. Human liver glycogen phosphorylase inhibitors bind at a new allosteric site. *Chem. Biol.* **2000**, *7*, 677−682.
(34) Chen, L.; Li, H.; Liu, J.; Zhang, L.; Liu, H.; Jiang, H. Discovering benzamide derivatives as glycogen phosphorylase inhibitors and their binding site at the enzyme. *Bioorg. Med. Chem.* **2007**, *15*, 6763−6774.
(35) Benltifa, M.; Vidal, S.; Gueyrard, D.; Goekjian, P. G.; Msaddek, M.; Praly, J. P. 1,3-Dipolar cycloaddition reactions on carbohydrate-based templates: synthesis of spiro-isoxazolines and 1,2,4-oxadiazoles as glycogen phosphorylase inhibitors. *Tetrahedron Lett.* **2006**, *47*, 6143−6147.
(36) Benltifa, M.; Hayes, J. M.; Vidal, S.; Gueyrard, D.; Goekjian, P. G.; Praly, J.-P.; Kizilis, G.; Tiraidis, C.; Alexacou, K.-M.; Chrysina, E. D.; Zographos, S. E.; Leonidas, D. D.; Archontis, G.; Oikonomakos, N. G. Glucose-based spiro-isoxazolines: a new family of potent glycogen phosphorylase inhibitors. *Bioorg. Med. Chem.* **2009**, *17*, 7368−7380.
(37) Dalvit, C.; Pevarello, P.; Tato, M.; Veronesi, M.; Vulpetti, A.; Sundstrom, M. Identification of compounds with binding affinity to proteins via magnetization transfer from bulk water. *J. Biomol. NMR* **2000**, *18*, 65−68.
(38) Mayer, M.; Meyer, B. Characterization of ligand binding by saturation transfer difference NMR spectroscopy. *Angew. Chem., Int. Ed.* **1999**, *38*, 1784−1788.
(39) Post, C. B. Exchange-transferred NOE spectroscopy and bound ligand structure determination. *Curr. Opin. Struct. Biol.* **2003**, 581−588.
(40) Stockman, B. J.; Dalvit, C. NMR screening techniques in drug discovery and drug design. *Prog. Nucl. Magn. Reson. Spectrosc.* **2002**, *41*, 187−231.
(41) Barelier, S.; Pons, J.; Gehring, K.; Lancelin, J. M.; Krimm, I. Ligand specificity in fragment-based drug design. *J. Med. Chem.* **2010**, *53*, 5256−5266.
(42) Martin, J. L.; Veluraja, K.; Ross, K.; Johnson, L. N.; Fleet, G. W.; Ramsden, N. G.; Bruce, I.; Orchard, M. G.; Oikonomakos, N. G.; Papageorgiou, A. C.; Leonidas, D. D.; Tsitoura, H. S. Glucose analogue inhibitors of glycogen phosphorylase: the design of potential drugs for diabetes. *Biochemistry* **1991**, *30*, 10101−10116.
(43) Murray, C. W.; Carr, M. G.; Callaghan, O.; Chessari, G.; Congreve, M.; Cowan, S.; Coyle, J. E.; Downham, R.; Figueroa, E.; Frederickson, M.; Graham, B.; McMenamin, R.; O'Brien, M. A.; Patel, S.; Phillips, T. R.; Williams, G.; Woodhead, A. J.; Woolford, A. J. Fragment-based drug discovery applied to Hsp90. Discovery of two lead series with high ligand efficiency. *J. Med. Chem.* **2010**, *53*, 5942−5955.
(44) Hajduk, P. J. Fragment-based drug design: how big is too big? *J. Med. Chem.* **2006**, *49*, 6972−6976.
(45) Bissantz, C.; Kuhn, B.; Stahl, M. A medicinal chemist's guide to molecular interactions. *J. Med. Chem.* **2010**, *53*, 5061−5084.
(46) Oikonomakos, N. G.; Schnier, J. B.; Zographos, S. E.; Skamnaki, V. T.; Tsitsanou, K. E.; Johnson, L. N. Flavopiridol inhibits glycogen phosphorylase by binding at the inhibitor site. *J. Biol. Chem.* **2000**, *275*, 34566−34573.
(47) Oikonomakos, N. G.; Skamnaki, V. T.; Tsitsanou, K. E.; Gavalas, N. G.; Johnson, L. N. A new allosteric site in glycogen phosphorylase b as a target for drug interactions. *Structure* **2000**, *8*, 575−584.
(48) Panjkovich, A; Daura, X Assessing the structural conservation of protein pockets to study functional and allosteric sites: implications for drug discovery. *BMC Struct. Biol.* **2010**, 10−19.
(49) Tsitsanou, K. E.; Skamnaki, V. T.; Oikonomakos, N. G. Structural basis of the synergistic inhibition of glycogen phosphorylase a by caffeine and a potential antidiabetic drug. *Arch. Biochem. Biophys.* **2000**, *384*, 245−254.